arXiv:astro-ph/0606427v1 18 Jun 2006

Capture Rates of Compact Objects by Supermassive Black Holes

José Antonio de Freitas Pacheco and Charline Filloux
Dpt. CASSIOPEE
Observatoire de la Côte d'Azur,
BP 429 06304 Nice (France). [*]

Tania Regimbau
Dpt. ARTEMIS
Observatoire de la Côte d'Azur,
BP 429 06304 Nice (France).[†]

(Dated: February 5, 2008)

Capture rates of compact objects were calculated by using a recent solution of the Fokker-Planck equation in energy-space, including two-body resonant effects. The fraction of compact objects (white dwarfs, neutron stars and stellar black holes) was estimated as a function of the luminosity of the galaxy from a new grid of evolutionary models. Stellar mass densities at the influence radius of central supermassive black holes were derived from brightness profiles obtained by Hubble Space Telescope observations. The present study indicates that the capture rates scale as $\propto M_{bh}^{-1.048}$, consequence of the fact that dwarf galaxies have denser central regions than luminous objects. If the mass distribution of supermassive black holes has a lower cutoff at $\sim 1.4\times10^6$ M$_\odot$ (corresponding to the lowest observed supermassive black hole mass, located in M32), then 9 inspiral events are expected to be seen by LISA (7-8 corresponding to white dwarf captures and 1-2 to neutron star and stellar black hole captures) after one year of operation. However, if the mass distribution extends down to $\sim 2\times10^5$ M$_\odot$, then the total number of expected events increases up to 579 (corresponding to $\sim$ 274 stellar black hole captures, $\sim$ 194 neutron star captures and $\sim$ 111 white dwarf captures).

PACS numbers:

I. INTRODUCTION

Dynamical evidences suggest that most, if not all elliptical galaxies and bulges of spirals host supermassive black holes (SMBHs) with masses ranging from $\sim 10^6$ M$_\odot$ up to few 10^9 M$_\odot$ [1, 2]. The most convincing example is the Milky Way, in which the orbital motion of stars around the radio source SgrA* indicates the presence of a massive compact object inside a radius less than 10^{-3} pc, having a mass of $\sim 2-3\times10^6$ M$_\odot$ [3].

These SMBHs are generally embedded in dense stellar environments and, consequently, they may capture stars which either will be promptly swallowed through the horizon or will inspiral by emitting gravitational waves. Interactions between stars and SMBHs in dense galactic nuclei have been the focus of many investigations in the past years, since these events are potential sources for the *Laser Interferometer Space Antenna* (LISA). The planned LISA noise spectral density is minimized around frequencies $\sim$ 3-30 mHz, setting the black hole mass interval of interest in the range $\sim 10^5 - 5\times10^6$ M$_\odot$. Main sequence stars, which dominate a given stellar population, will be disrupted by tidal forces if the black hole mass is less than $\sim 2\times10^8$ M$_\odot$, since the Roche limit will be inside their gravitational radius. Thus, only the capture of compact objects like white dwarfs, neutron stars and stellar black holes may produce a gravitational signal relevant for LISA.

Inside the influence radius r_{bh} of the SMBH, the orbits are dominated by the gravitational potential of central hole but are perturbed by nearby stellar encounters. This means that the total mass under the form of stars inside r_{bh} is less than the mass of the SMBH and that the radius of this dynamical sphere of influence can be estimated by equating the potential energy of the SMBH, GM_{bh}/r_{bh}, to the kinetic energy of the stars, $\frac{3}{2}\sigma_{1D}^2$ [4]. In the one hand, stellar-stellar interactions may produce important variations in energy and angular momentum per orbital period, leading to a prompt capture of the star if the resulting angular momentum is less than a critical value $J_{crit} = 4GM_{bh}/c$, for a Schwarzschild black hole. The phase-space volume defined by $J \leq J_{crit}$ is dubbed the "loss cone" [5, 6, 7] and the infall of these stars in eccentric orbits onto the SMBH is set by the rate at which relaxation processes repopulate the loss cone orbits. On the other hand, stars in tightly bound orbits may undergo a "diffusion" in J-space with a small step size ΔJ per orbital period. In this case, they lose angular momentum mainly by gravitational radiation, susceptible to be detected by LISA. In the absence of the central SMBH, the diffusion-in is balanced by the diffusion-out of the "loss cone" and the net flow is zero, which is not the case when a secular decay of low angular momentum orbits occurs due to gravitational radiation.

Due to the complexity of the energy and angular momentum transfer, predicted capture rates found in the literature may vary by orders of magnitude. An early

---

[*] Electronic address: pacheco@obs-nice.fr, filloux@obs-nice.fr
[†] Electronic address: regimbau@obs-nice.fr

Monte Carlo simulation of the stellar random walk in J-space was performed by [8], using parameters appropriate for the core of the dwarf elliptical M32, resulting in a event rate of 1.9×10^{-8} yr^{-1} if compact stars are assumed to represent 10% of the total stellar population. Similar simulations were performed by [9] but for parameters appropriate to the galactic center. In this case, the capture rate of white dwarfs was found to be $\sim 2-3\times10^{-7}$ yr^{-1} and those of neutron stars and black holes about one order of magnitude lower. Analytical estimates of the capture rate were performed by [10], who have found, in particular for M32, a rate comparable to that obtained by [8]. Analytical and Monte Carlo methods were adopted by [11] and from their approach a typical event rate of few $\times10^{-9}$ yr^{-1} per galaxy was derived.

As mentioned above, the capture rate is grossly given by the ratio between the number of stars inside the black hole influence radius and the two-body relaxation time at this position [5, 7]. The relaxation time is essentially a measure of the timescale required for uncorrelated two-body interactions to change the original energy E of a given star by $\Delta E\sim E$. This timescale is also comparable to that required for the specific angular momentum to change by an amount comparable to the maximum angular momentum for that energy, corresponding to circular orbits. In dynamical systems where the potential induces precessing orbits, as long as the precession timescale (time required to change the argument of the periapse by π) is larger than the orbital period, two-body interactions last longer and can be imagined as "correlated". The consequences of coherent interactions were recently discussed by [12], who have concluded that the steady stellar flow may increase by almost one order of magnitude in comparison with a current of stars driven only by non-resonant relaxation.

In this work the capture rate of compact objects by SMBHs present in the center of early-type (E+S0) and bulges of disky galaxies was estimated from the steady current solution of the Fokker-Planck equation in energy-space obtained by [12], including resonant and non-resonant interactions. For a sample of E/S0 galaxies, the stellar density at the influence radius was estimated from the brightness profile derived from Hubble Space Telescope (HST) observations, permitting the derivation of scaling relations either between the capture rate and the total luminosity of the "hot" stellar component of the galaxy or the mass of the central SMBH. The present analysis indicates that dwarf-compact galaxies, besides hosting SMBHs with masses in the range of interest for LISA, have the highest capture rates since their cores have stellar densities higher than giant ellipticals. Convolving with the mass distribution of SMBHs, the expected number of events to be detected by LISA after one year of operation was estimated. A conservative estimate, including only galaxies brighter than M32, indicates that about 9 events are expected to be detected by LISA. If objects as faint as $M_B=-14$ are supposed to host SMBHs, extending the mass integration down to $\sim 2\times10^5\ M_\odot$, the expected number of events increases dramatically to values around 580. This paper is organized as follows: in Section II, the capture rate and the astrophysical parameters required for its calculation are discussed; in Section III, the maximum redshift at which an inspiral capture can be detected by LISA is computed as a function of the black hole mass; in Section IV, using the previous results, estimates of the number of events expected to be detected by LISA in one year of observations are given and finally, in Section V, our main conclusions are summarized.

II. THE CAPTURE RATE

As discussed in [12], resonant relaxation may increase the inspiral rate by almost one order of magnitude relative to rates predicted by assuming only uncorrelated two-body interactions. This is a consequence of the fact that symmetries in the gravitational potential restrict the evolution of the orbits [13], increasing the time interval during which stars exert mutual torques. In the present work the results obtained by [12] are used to estimate the capture rate in elliptical and bulges of spiral galaxies. Notice that the solution obtained by [12] when applied to the galactic center predicts a capture rate of white dwarfs of about 1.2×10^{-7} yr^{-1}, in agreement with the results derived from Monte Carlo simulations by [9].

The capture rate of compact objects $R_{\rm co}$, including both resonant and non-resonant relaxation is given by

$$R_{co}=\frac{8\pi^2}{3\sqrt{2}}\rho_{bh}^2 r_{bh}^3\frac{G^2\ln\Lambda}{\sigma_{bh}^3}f_{co}Q(x_{gw}) \qquad (1)$$

where $\rho_{\rm bh}=\rho(r_{\rm bh})$ is the stellar mass density at the influence radius $r_{bh}=2GM_{bh}/3\sigma_{bh}^2$, Λ is the "Coulomb factor" expressing the ratio between the maximum and the minimum impact parameter of stellar interactions inside the influence radius, σ_{bh} is the line-of-sight velocity dispersion at the influence radius and f_{co} is the fraction of compact objects of the stellar population present in central region of the galaxy. $Q(x)$ is the dimensionless net steady rate at which stars flow to energies larger than x. The dimensionless energy is defined by $x=E/\sigma_{bh}^2$, where E is the binding energy of the star per unit of mass. Only stars with energies $E\geq E_{\rm gw}$ can inspiral into the SMBH without being scattered to a wider orbit of lower energy. The critical energy E_{gw} can be estimated by equating the inspiral timescale due to gravitational radiation losses with the timescale required for collisions produce a variation ΔJ in the angular momentum of the order of J, [11]. In this case one obtains for the dimensionless energy

$$x_{gw}=2.4\times10^{-5}\frac{M_6^{3/2}(\rho_{bh}\ln\Lambda)^{2/3}}{\sigma_{200}^4} \qquad (2)$$

where M_6 is the black hole mass in units of 10^6 M$_\odot$, σ_{200} is the line-of-sight velocity dispersion in units of 200 km/s and the stellar density at the influence radius is given in $\mathrm{M}_\odot\mathrm{pc}^{-3}$.

The dimensionless flow rate $Q(x)$ is derived from the Fokker-Planck energy equation including sink terms due to resonant and non-resonant relaxation. The numerical solution derived by [12] depends on a factor χ, which characterizes the efficiency of the resonant relaxation. Here the conservative value $\chi = 1$ is adopted. In order to facilitate the numerical computations, the solution derived by [12] was fitted by a polynomial accurate enough for our purposes, valid in the range $1 \leq x \leq 550$, e.g.,

$$\log Q(x) = -0.4906 - 0.4545\log(x) + 0.3826\log^2(x) - 0.2146\log^3(x) \quad (3)$$

A. The fraction of compact stars

In eq.1, besides the stellar density, the fraction of compact objects f_{co} is one of the astrophysical parameters required to compute the capture rate. For a given stellar population, the fraction of white dwarfs, neutron stars and black holes depends on *the age and on the initial mass function* (IMF).

If the spectrophotometric indices of elliptical galaxies are interpreted in terms of single stellar populations, then ages ranging from few Gyr up to tens Gyr are obtained [14, 15]. Elliptical galaxies are certainly not single stellar systems in spite of the fact that the bulk of their stars was formed in a short lapse of time. The build up of chemical elements requires successive stellar generations, indicating that those systems are constituted by a population mix. Multi-population models point to a small age spread around 12 Gyr [16]. A second point to be emphasized, consequence of these multi-population models, is that the IMF must be flatter than the usual Salpeter's law in more massive galaxies, in order to explain the trend of the α-elements abundance ratio with the luminosity of the galaxy [16, 17]. As a consequence, the relative number of neutron stars and stellar black holes in luminous galaxies are higher than in dwarf objects.

Here an up-graded version of the grid of models by [16] was used to estimate the fraction of compact stars in elliptical galaxies of different masses. Models with an IMF of the form $\xi(m) \propto m^{1+x}$ were developed and were required to reproduce the observed trends in the color-magnitude diagram, (U-V) versus M_V, as well as in the plane of the indices Mg_2 and $< Fe >$. This was obtained by adjusting free parameters like the star formation efficiency and the exponent x of the IMF. Stars with masses m lower than 9.0 $\mathrm{M}_\odot$ give origin to a white dwarf of mass $m_{wd} = 0.116m + 0.455$, while progenitors in the range 9-50 $\mathrm{M}_\odot$ were supposed to give origin to a neutron star of mass 1.4 $\mathrm{M}_\odot$. Above 50 $\mathrm{M}_\odot$ stars are supposed to produce a black hole of 10 $\mathrm{M}_\odot$. The upper limit of ~ 50 $\mathrm{M}_\odot$ to form a black hole is consistent with data on X-ray pulsars present in binary systems like Wray 977 [18] and Westerlund 1 [19].

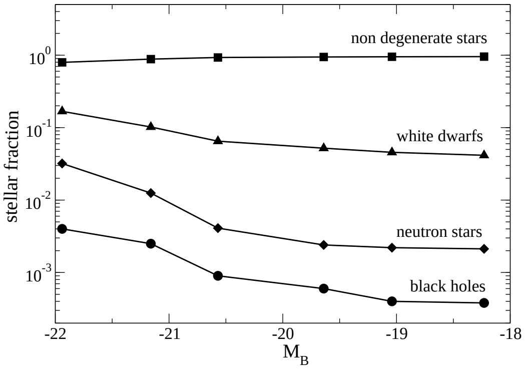

FIG. 1: Theoretical fractions of non-degenerate stars and of compact objects as a function of the absolute magnitude of the galaxy

The expected fraction of non-degenerate stars (essentially main sequence stars), white dwarfs, neutron stars and black holes as a function of the absolute magnitude M_B of the galaxy is shown in fig.1. In very massive galaxies with $M_B \approx -22.0$, the fraction of white dwarfs may reach values as high as 16%, whereas the fraction of neutron stars and black holes attain values of about 3.2% and 0.4% respectively. These results will be used in our capture rate estimates.

B. The stellar density

Another important astrophysical quantity required to compute the inspiral rate from eq.1 is the stellar density at the influence radius. Near the center, the surface brightness along a given axis may be written as

$$I(r) = I_0 + I_1 r^2 + \mathcal{O}(r^4) \quad (4)$$

where r is the projected distance from the center. According to [23], a galaxy satisfying the above relation can be said to have an "analytic core" and its core radius R_c is defined by the condition $I(R_c) = \frac{1}{2}I(0)$. However, HST data have shown that real cores are not analytic but display shallow power-law cusps into the resolution limit, which brightness can be fitted by the so-called Nuker law [24], e.g.,

$$I(r) = 2^{(\beta-\gamma)/\alpha} I_b(\frac{r_b}{r})^\gamma [1 + (\frac{r}{r_b})^\alpha]^{(\gamma-\beta)/\alpha} \quad (5)$$

where I_b, r_b, α, β and γ are fitting parameters. According to [20], essentially two types of galaxies can be distinguished on the basis of the aforementioned parameters: a) "core" galaxies, which have an inner logarithmic slope $| d\log I/d\log r |< 0.3$ and b) "power law" galaxies, which show a fairly steep brightness profile for $r < r_b$.

The former class includes luminous objects whereas the later includes fainter galaxies. These properties are fundamental to understand the stellar environment in which the central black hole is embedded.

Once the intensity profile is known, the luminosity density ρ_L can be derived by inverting an Abel integral [22], e.g.,

$$\rho_L(R) = -\frac{1}{\pi}\int_R^\infty \frac{(dI(r)/dr)}{\sqrt{r^2-R^2}}dr \tag{6}$$

and the stellar mass density can be obtained by multiplying the luminosity density by the mass-to-luminosity ratio $\Upsilon_V = \mathcal{M}/L_V$ in solar units. From our models,

$$\log\Upsilon_V = -1.148 - 0.0956M_V \tag{7}$$

The stellar density at the influence radius was computed numerically using eqs.5, 6 and 7. The parameters defining the brightness profile as well as absolute magnitudes were taken from reference [24], corrected for a Hubble constant $H_0 = 70$ kms^{-1}Mpc^{-1}, adopted in the present work. Black hole masses required to compute the influence radius, when available were taken from [26, 27] or computed from the relation

$$M_{bh} = 1.4\times10^8\sigma_{200}^{4.26}\,\mathrm{M}_\odot \tag{8}$$

which is slightly different from the original fits derived by [28] or [27], since here only E and S0 galaxies were included (bulges of spirals were excluded from the fit).

Fig.2 shows the stellar density at the influence radius as a function of the absolute magnitude of the galaxy. This plot just confirms the known fact that dwarf ellipticals have central densities considerably higher than bright E-galaxies, which is essentially a consequence of "power-law" profiles present in the former objects and the existence of a fundamental plane, correlating structural parameters like the central velocity dispersion, the effective brightness and the effective radius. As a corollary, SMHBs with masses around $\sim 10^{5-6}$ M$_\odot$ are always embedded in denser stellar environments, thus having higher capture rates, than those surrounding SMBHs with masses around 10^{8-9} M$_\odot$, which have capture rates one or two orders of magnitude lower.

C. The estimated inspiral rates

For galaxies included in the sample studied by [24], capture rates were calculated from eq.1, using the fraction of compact objects, stellar density and influence radius estimated according to the procedure described above. The resulting capture rate of white dwarfs scales with the luminosity of the galaxy as

$$R_{wd} = \frac{8.31\times10^4}{(L_B/L_{B,\odot})^{1.31}}\ \mathrm{yr}^{-1} \tag{9}$$

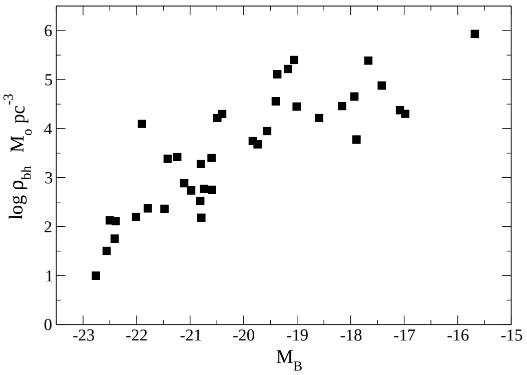

FIG. 2: Stellar densities at the influence radius as a function of the absolute B-magnitude for galaxies included in the sample by Faber et al. [24]. Absolute magnitudes were taken from LEDA database [25].

whereas the scaling with the SMBH mass is

$$R_{wd} = \frac{0.86}{(M_{bh}/\mathrm{M}_\odot)^{1.048}}\ \mathrm{yr}^{-1} \tag{10}$$

The capture rate of neutron stars and stellar black holes can be obtained by multiplying the equations. above respectively by 0.0511 and 0.00916. In spite of these small rates, the gravitational signal resulting from the capture either of a neutron star or a stellar black hole can be detected much further away than that resulting from the capture of a white dwarf, which makes their detection rate comparable, as we will demonstrate later. Notice that due to the square dependence on the stellar mass density in eq.1, the capture rate *decreases* with increasing SMBH masses, since more massive holes live in less dense stellar environments.

If one assumes that the relaxation timescale t_R is comparable to the mean population age, e.g., 12 Gyr, then the stellar density and the velocity dispersion at r_{bh} must satisfy

$$\rho \approx 0.154\sigma_{1D}^{2.905}\ \mathrm{M}_\odot\mathrm{pc}^{-3} \tag{11}$$

where σ_{1D} is given in km/s. On the other hand, densities at the influence radius derived in the previous section and the line-of-sight velocity dispersion are approximately related as

$$\rho \approx 1.44\times10^{15}\sigma_{1D}^{-5.137}\ \mathrm{M}_\odot\mathrm{pc}^{-3} \tag{12}$$

From these two relations, in order that $t_R \leq 12$ Gyr, one must have $\sigma_{1D} \leq 100$ km/s and/or $\rho_{bh} \geq 9.0\times10^4$ M$_\odot$pc^{-3}. This means that only galaxies *fainter* than $M_B = -18$ have relaxation timescales less or equal 12 Gyr and can satisfy the steady conditions required by eq.1. Galaxies brighter than this limit are not able to refill their "loss cones" within a Hubble time and probably have a non steady inspiral flow. Therefore, we will restrict the application of eq. 9 or eq. 10 to objects fainter than the aforementioned limit, which corresponds to galaxies hosting central black holes with masses around $\sim 8 \times 10^6$ M$_\odot$.

Eqs. 9, 10 are valid, in principle, only for early-type galaxies. However, here they will be also applied to bulges. Bulges constitute, in general, an extension of low luminosity ellipticals. They follow quite well the $Mg_2 - \sigma_{1D}$ diagram of ellipticals [29], the SMBHs present in the center of bulges follow approximately the same $M_{bh} - \sigma_{1D}$ relation obeyed by early-type galaxies (but having probably a slightly steeper slope although more data are needed to confirm such a trend [21]) and stellar densities derived at the influence radius, at least for two cases, are in agreement with the results displayed in fig.2. These are the bulges of the Milky Way, if we use the results by [30] and that of NGC 1316, if we use the procedure described above and data from [24].

III. THE REDSHIFT SPACE PROBED BY LISA

Estimates of the number of events expected to be detected by LISA demand a previous evaluation of the volume of the universe probed by the detector or, in other words, an evaluation of the maximum redshift at which a given inspiral gravitational signal can be seen.

For the inspiral up to the last stable orbit (LSO), theoretical templates of the waveform $h(t)$ will probably be available and the method of matched filtering can be used. In this case, the resulting signal-to-noise ratio (SNR) is [31]

$$(\frac{S}{N})^2 = 4\int_0^\infty d\nu \frac{|(\tilde{h}_+(\nu)F_+(\nu) + \tilde{h}_\times(\nu)F_\times(\nu))|^2}{S_n(\nu)} \quad (13)$$

where $S_n(\nu)$ is the spectral density of the strain noise of the detector and the Fourier transform of the two polarization amplitudes, $\tilde{h}_+$ and $\tilde{h}_\times$, depends on the source orientation, on the detector beam pattern functions F_+ and $F_\times$, on the polarization and on the source sky location. Averaging over source positions and orientations one obtains [32]:

$$(\frac{S}{N})^2_{\rm rms} = 2\int_0^\infty d\nu \frac{S_h(\nu)R(\nu)}{S_n(\nu)} \quad (14)$$

where the response function of the detector averaged over sky directions and polarizations can be expressed as [32]:

$$R(\nu) = \int \frac{d\Omega}{4\pi} \sum_{A=+,\times} F^{A*}(\hat{\Omega},\nu)F^A(\hat{\Omega},\nu) \quad (15)$$

On the other hand, the planned LISA sensitivity is usually given in terms of the quantity

$$|\, \tilde{h}_{eff}(\nu)\, |^2 = (\frac{S_n(\nu)}{R(\nu)}) \quad (16)$$

The spectral density of the gravitational signal is given by [31]

$$S_h(\nu) = \frac{1}{2}\frac{G}{\pi^2 c^3}\frac{(1+z)^2}{d_L^2}\frac{1}{\nu^2}\frac{dE}{d\nu_e}((1+z)\nu) \quad (17)$$

where ν and ν_e are respectively the gravitational wave frequencies at the observer's frame and at the source related by $\nu_e = (1+z)\nu$, $d_L = (1+z)r(z)$ is the distance luminosity with $r(z)$ being the proper distance defined by

$$r(z) = \frac{c}{H_0}\int_0^z \frac{dz'}{E(\Omega_i, z')} \quad (18)$$

with

$$E(\Omega_i, z) = \sqrt{\Omega_v + \Omega_m(1+z)^3} \quad (19)$$

where $\Omega_v = 0.7$ and $\Omega_m = 0.3$ are respectively the present values of the density parameters due to vacuum and matter (baryonic + non-baryonic) adopted in the present work, in agreement with the "concordance" model ([33]). In eq.17, the spectral energy density of the source in the quadrupole approximation, which is adequate to estimate the SNR obtained from matched filtering

$$\frac{dE}{d\nu_e} = \frac{(G\pi)^{2/3}}{3}\mu M^{2/3}\nu_e^{-1/3} \quad (20)$$

where the reduced mass $\mu \approx m_{co}$ and the total mass $M \approx M_{bh}$.

Combining eqs.17, 20 and 16 into 14, one obtains

$$(\frac{S}{N})^2_{\rm rms} = \frac{1}{3\pi^{4/3}}\frac{Gm_{co}}{c^3}\frac{(GM_{bh})^{2/3}}{r^2(z)(1+z)^{1/3}}\mathcal{I}_\nu \quad (21)$$

where

$$\mathcal{I}_\nu = \int_{\nu_{min}/(1+z)}^{\nu_{max}/(1+z)} \frac{\nu^{-7/3}}{|\, \tilde{h}_{eff}(\nu)\, |^2} d\nu \quad (22)$$

The upper limit of the above integral corresponds to the frequency associated to the LSO, corrected for the observer's frame, e.g.,

$$\nu_{max} = \frac{c^3}{\sqrt{216}\pi G M_{bh}} = \frac{0.004384}{M_6}\ Hz \quad (23)$$

For the lower limit we take the frequency corresponding to about one year before arrival at the LSO, namely,

$$\nu_{min} = \frac{\nu_{max}}{(1 + \frac{0.25 m_{co}}{M_6^2})^{3/8}} \quad (24)$$

where m_{co} is in solar units and M_6 is in units of 10^6 $M_\odot$.

Following the convention adopted in the LISA community, the detectability threshold was settled to be $S/N = 5$ and from the numerical solution of eq.21 one obtains, for a given compact object of mass m_{co}, the maximum redshift as function of the SMBH mass M_{bh}.

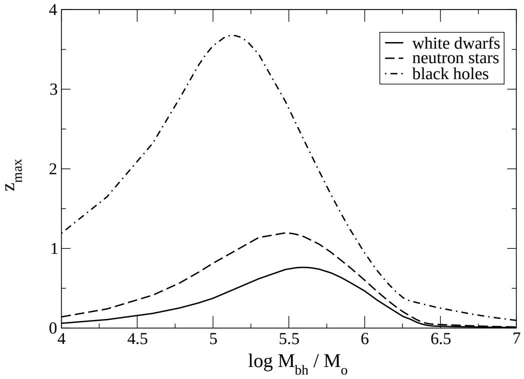

FIG. 3: Maximum redshift (z_{max}) at which a gravitational signal resulting from an inspiral capture can be detected by LISA operating as a Michelson interferometer. A signal-to-noise ratio equal to 5 was adopted and the WD-WD galactic binary confusion noise was included.

The effective noise budget sensitivity (see eq.16) used in the calculations refers to a standard Michelson configuration [34], including the contribution of the galactic binary WD-WD confusion noise [35, 36]. The resulting curves for white dwarfs ($m_{wd} = 0.7$ M$_\odot$), neutron stars ($m_{ns} = 1.4$ M$_\odot$) and stellar black holes ($m_{bh} = 10$ M$_\odot$) are shown in fig.3. The farthest inspiral signal resulting from the capture of a white dwarf corresponds to a redshift $z \sim 0.76$ and a SMHB mass of about 3.9×10^5 M$_\odot$, that resulting from the capture of a neutron star corresponds to $z \sim 1.19$ and a SMBH of 3.1×10^5 M$_\odot$ whereas the signal resulting from the capture of a stellar black hole by a SMBH of mass 1.3×10^5 M$_\odot$ can be seen up to $z \sim 3.67$.

IV. THE EXPECTED NUMBER OF EVENTS

Once the maximum redshift z_{max} at which a given inspiral signal can be detected is calculated, the expected number of events Γ_{co} in a time interval T can be estimated from the equation

$$\Gamma_{co} = T\int_{M_1}^{M_2}\frac{R_{co}(M_{bh})}{(1+z)}\frac{d\mathcal{N}(M_{bh},z)}{dM_{bh}}dM_{bh}\int_0^{z(M_{bh})}\frac{dV}{dz}dz \qquad (25)$$

In this equation, $R_{co}(M_{bh})$ is the capture rate of a given compact object as a function of the black hole mass, as calculated in Section II.B and the term (1+z) in the denominator corrects for time dilation as the universe expands. Evolutionary effects which may affect the mass of the central black hole and/or the nearby stellar distribution were neglected in the present approach but are under investigation. For the SMBH mass distribution, the results by [37] were used. These authors derived for the local mass distribution function

$$\frac{d\mathcal{N}(M_{bh},z)}{dM_{bh}} = \frac{\theta_* h^3}{M_0}(\frac{M_0}{M_{bh}})^{1-\gamma}e^{-(M_{bh}/M_0)^{\epsilon}}(1+z)^3 \qquad (26)$$

where the parameters θ_*, M_0 and γ where calculated for the different morphological types, using the luminosity distribution functions by [38]. The parameter $\epsilon = 0.8 \pm 0.1$ depends on the slopes of the adopted $M_{bh} - \sigma_{1D}$ and $L - \sigma_{1D}$ relations. Since the luminosity function concerns the “total” galaxy luminosity, in the case of bulges of spirals the derivation of the black hole mass distribution depends on the relative bulge-to-total luminosity ratio for the different morphological types. Since average values for the various morphological types have a considerable dispersion, this introduces an important source of uncertainty in the parameters corresponding to disky galaxies. In above equation, the conservation of the number of galaxies within the comoving volume was included but no other evolutionary effect. The comoving volume in eq. 25 is given by

$$\frac{dV}{dz}dz = 4\pi r^2(z)\frac{c}{H_0}\frac{dz}{E(\Omega_i,z)} \qquad (27)$$

In the second integral of eq.25, the upper limit M_2 corresponds to the critical luminosity beyond which the relaxation time is larger than 12 Gyr and, consequently, a steady stellar current can not be established. The conversion of luminosities into SMBH masses was performed through the relation

$$\log M_{bh}/M_\odot = -0.835 - 0.439 M_B \qquad (28)$$

If, as we shall see, our results are practically independent on the assumed upper limit M_2, the situation is quite different concerning the lower limit M_1, since the capture rate increases for these less massive black holes. The lower mass cutoff is uncertain since up today observational searches for intermediate-mass black holes have been discouraging. Presently, the smallest known central black hole is located in the dwarf elliptical M32, having a mass $\sim 1.4 \times 10^6$ M$_\odot$ ([26]). A conservative estimate of the number of events can be obtained if this value is taken as the minimum mass. From an observational point of view, the existence of SMBHs with masses lower than the above limit is still controversial. Analyses of dynamical data on the dwarf galaxies M33 [39, 40] and NGC 205 [21] lead to robust upper limits respectively of $\sim 3 \times 10^3$ M$_\odot$ and $\sim 4 \times 10^4$ M$_\odot$ to the putative black holes living in the center of these objects. Moreover, searches for intermediate mass black holes in dwarf-spheroidal satellites of the Milky Way have also been negative [41]. However, these small galaxies were captured by our Galaxy and, in the process, collective effects may transfer energy to their central black holes enough to move them far away from the core, escaping from detection. If direct dynamical evidences of SMBHs in such a mass range are missing, indirect signals of their presence in narrow-line Seyfert-1 nuclei exist. Using the line width-luminosity-mass scaling relation established for broad-line AGNs, SMBH masses were estimated by [42] for a sample of 19 galaxies, all in the range 8×10^4 up to 8×10^6 $M_\odot$. Therefore, an "optimistic" estimate was also performed by assuming that central black black holes are present at least in compact dwarf galaxies and bulges brighter than $M_B = -14$, since their cores follow quite well the M_{bh}-luminosity relation [43]. Using eq. 28, this luminosity corresponds to a SMBH of about 2×10^5 $M_\odot$. Such a lower limit were used for "optimistic" estimates of the capture rate of neutron stars and stellar black holes, since for white dwarfs the adopted lower limit was slightly higher $\sim 6 \times 10^5$ $M_\odot$, corresponding to the mass for which the tidal radius is comparable to the gravitational radius. The results of our computations indicate that in the *conservative* case, 9 inspiral events are expected to be detected by LISA. In this case, the estimated probability to have a white dwarf capture is 84.5% and those for the capture of a neutron star or a stellar black hole are 8.0% and 7.5% respectively. Early-type galaxies are expected to contribute to about 53.8% of the total number of events, Sa+Sb bulges contribute to about 26.9% and Sc bulges contribute to about 19.3%.

If the lower mass integration limit is reduced down to 2×10^5 $M_\odot$, there is a dramatic increase in the expected number of events. This occurs because the capture rate increases for lower SMBH masses as well as the volume of the universe probed by LISA (see fig.3). In this "optimistic" case, the expected number of events is 579. The contribution of the different compact objects is now rather different: stellar black holes are expected to represent about 47.4% of the total number of events, neutron stars will contribute to about 33.5% and white dwarfs, to about 19.1%. The contribution of the different morphological types will be practically the same as before, e.g., E+S0 will contribute to about 53.2%, Sa+Sb, to about 20.5% and Sc to about 26.3%.

V. CONCLUSIONS

Diffusion in energy-space of stars under the gravitational influence of a supermassive black hole was recently considered in [12], including phenomenologically a term in the Fokker-Planck equation, corresponding to two-body resonant relaxation. These results were used to estimate the capture rate of compact objects in a sample of early-type galaxies.

From a new grid of evolutionary models for early-type galaxies, including a variable initial mass function, the fraction of white dwarfs, neutron stars and stellar black holes was derived as a function of the luminosity (mass) of the galaxy, as well as the (stellar) mass-to-luminosity ratio, quantities necessary to compute capture rates. The later was used to estimate stellar mass densities by inversion of brightness profiles of a sample of early-type objects, obtained from HST observations. The analysis of these results indicates that the capture rate decreases for high luminosity galaxies, which harbor the most massive black holes. This is a consequence that luminous E-galaxies have cored density profiles whereas fainter objects have in general "power-law" profiles, providing a denser stellar environment to their hosts.

Interpretation of colors and metallicity indices of early-type galaxies by evolutionary models indicates mean population ages of about 12 Gyr with a dispersion of about 2 Gyr. If dynamical ages are comparable, then only systems fainter than $M_B = -18$ are able to refill their loss cones and maintain a steady stellar current. Such a luminosity corresponds to a SMBH mass of $\sim 8 \times 10^6$ $M_\odot$ and constitutes a limit for the application of steady solutions of the Fokker-Planck equation.

Extending our results to bulges of spirals, face their similarity to E-galaxies, the expected number of events to be detected by LISA in one year of operation was estimated. Two situations were considered: in the first, a conservative estimate was performed by restricting the integration over masses in the range defined by the aforementioned upper limit and the lower limit defined by the lowest SMBH mass detected up today, e.g., the one located in M32. A second and a more optimistic estimate, extends the lower mass limit down to 2×10^5 $M_\odot$ corresponding to a luminosity of $M_B = -14.0$. The core of these compact dwarf galaxies, able to host those undetected up to now black holes, follow the $M - \sigma$ relation [43] defined by brighter galaxies and bulges, which is encouraging. In this case, the resulting expected number of events is 579. The inclusion of SMBHs with masses lower than few 10^6 $M_\odot$ increases not only the capture rate but also increases the volume "seen" by the detector (see fig.3). In the conservative case, between 7-8 events, probably associated to the capture of white dwarfs and 1-2 events, probably associated to the capture of neutron stars and stellar black holes are expected to be seen by LISA after one year of operation. Reducing the lower mass limit, events associated to the capture of stellar black holes will be dominant (~ 274), followed by those associated to the capture of neutron stars (~ 194) and white dwarfs (~ 111). These aspects associated with the number of events and the distribution of the different captured compact objects reveal the potential of gravitational waves as tool for astrophysics, in particular for scenarios of SMBH formation.

However, it should be emphasized that the present estimates neglect possible evolutionary effects. If mean population ages of early-type galaxies and bulges are ~ 12 Gyr, this means that they were already assembled around $z \sim 3.6$, which corresponds practically to the maximum redshift that an inspiral gravitational signal produced by the capture of a stellar black hole by a SMBH of mass $\sim 1.3 \times 10^5$ $M_\odot$ can be detected by LISA with a SNR = 5. No important variations are expected to occur in the central region of the galaxy as a consequence of the capture of compact objects in such a timescale. However, non-degenerate stars will diffuse-in the influence radius and will be destroyed by tidal forces, representing a mass consumption in a timescale of 12 Gyr which may be comparable to the that of a $\sim 2 \times 10^5$ $M_\odot$ black hole. This process will modify slowly the central density profile and the SMBH mass. Moreover, hosting dark halos are continuously accreting mass [44], affecting the mass history of central black hole and the structure of the galaxy as well. These problems are presently under investigation through cosmological numerical simulations and will be reported in a future paper.

---

[1] D. Richstone et al., Nature 395, 14 (1998)
[2] J. Kormendy and K. Gebhardt, in Supermassive Black Holes in Galactic Nuclei, 20th Texas Symposium on Relativistic Astrophysics, ed. H. Martel & J.C. Wheeler, 363 (2001)
[3] R. Schodel et al., Nature 419, 694 (2002)
[4] P.J.E. Peebles, Gen.Rel.Grav. 3, 63 (1972)
[5] J.N. Bahcall and R.A. Wolf, ApJ 209, 214 (1976)
[6] J.N. Bahcall and R.A. Wolf, ApJ 216, 883 (1977)
[7] A.P. Lightman and S.L. Shapiro, ApJ 211, 244 (1977)
[8] D. Hils and P. Bender, ApJ 445, L7 (1995)
[9] M. Freitag, ApJ 583, L21 (2003)
[10] S. Sigurdsson and M.J. Rees, MNRAS 284, 318 (1997)
[11] C. Hopman and T. Alexander, ApJ 629, 362 (2005)
[12] C. Hopman and T. Alexander, ApJ, in press (2006); astro-ph/0601161
[13] S. Tremaine, ApJ 625, 143 (2005)
[14] S.C. Trager, S.M. Faber, G. Worthey and J.J. Gonzáles, AJ 120, 165 (2000)
[15] D. Thomas, C. Maraston, R. Bender and C. Mendes de Oliveira, ApJ 621, 673 (2005)
[16] T.P. Idiart, R. Michard and J.A. de Freitas Pacheco, A&A 398, 949 (2003)
[17] F. Matteucci and A. Tornambè, A&A 185, 51 (1987)
[18] L. Kaper et al., A&A 300, 446 (1995)
[19] M.P. Muno et al., ApJ 636, 41 (2006)
[20] T.R. Lauer et al., AJ 110, 2622 (1995)
[21] M. Valluri, L. Ferrarese, D. Merritt and C.L. Joseph, ApJ 628, 137 (2005)
[22] K. Gebhardt et al., AJ 112, 105 (1996)
[23] D.O. Richstone and S. Tremaine, AJ 92, 72 (1986)
[24] S. Faber et al., AJ 114, 1771 (1997)
[25] LEDA, Lyon Extragalactic Database, http://leda.univ-lyon1.fr/
[26] D. Merrit and L. Ferrarese, MNRAS 320, L30 (2001)
[27] S. Tremaine et al., ApJ 574, 740 (2002)
[28] D. Merrit and L. Ferrarese, ApJ 547, 140 (2001)
[29] T.P. Idiart, J.A. de Freitas Pacheco and R.D.D. Costa, AJ 112, 254 (1996)
[30] R. Genzel et al., ApJ 594, 812 (2003)
[31] E.E. Flanagan and S.A. Hughes, PRD 57, 4535 (1998)
[32] N.J. Cornish, PRD 65, 022004 (2001)
[33] D.N. Spergel et al., ApJS 148, 175 (2003)
[34] P. Bender et al., LISA Pre-Phase A Report (1998)
[35] D. Hils, P. Bender and R.F. Webbink, ApJ 360, 75 (1990)
[36] S.L. Larson, *Online Sensitivity Curve Generator*, located at http://www.srl.caltech.edu~shane/sensitivity/; S.L. Larson, W.A. Hiscock and R.W. Hellings, PRD 62, 062001 (2000)
[37] M.C. Aller and D. Richstone, AJ 124, 3035 (2002)
[38] R.O Marzke, M.J. Geller, J.P. Huchra and H.G. Corwin, ApJ. 108, 437 (1994)
[39] D. Merritt, L. Ferrarese and C.L. Joseph, Science 293, 1116 (2001)
[40] K. Gebhardt et al., AJ 122, 2469 (2001)
[41] T.J. Maccarone, R.P. Fender and A.K. Tzioumis, MNRAS 356, L17 (2005)
[42] J.E. Greene and L.C. Ho, ApJ 610, 722 (2004)
[43] E.H. Wehner and W.E. Harris, ApJ in press,astro-ph/0603801
[44] S. Peirani, R. Mohayaee and J.A. de Freitas Pacheco, MNRAS 348, 921 (2004)